

# Accuracy of entanglement detection via artificial neural networks and human-designed entanglement witnesses

Jan Roik,<sup>1,\*</sup> Karol Bartkiewicz,<sup>2,1,†</sup> Antonín Černoč,<sup>1,‡</sup> and Karel Lemr<sup>1,§</sup>

<sup>1</sup>*RCPTM, Joint Laboratory of Optics of Palacký University and Institute of Physics of Czech Academy of Sciences, 17. listopadu 12, 771 46 Olomouc, Czech Republic*

<sup>2</sup>*Faculty of Physics, Adam Mickiewicz University, PL-61-614 Poznań, Poland*

(Dated: November 9, 2021)

Detection of entangled states is essential in both fundamental and applied quantum physics. However, this task proves to be challenging especially for general quantum states. One can execute full state tomography but this method is time demanding especially in complex systems. Other approaches use entanglement witnesses, these methods tend to be less demanding but lack reliability. Here, we demonstrate that ANN – artificial neural networks provide a balance between both approaches. In this paper, we make a comparison of ANN performance against witness-based methods for random general 2-qubit quantum states without any prior information on the states. Furthermore, we apply our approach to real experimental data set.

## I. INTRODUCTION

Quantum entanglement is an intriguing phenomenon described almost a century ago by Schrödinger, Einstein, Podolsky, and Rosen [1, 2]. Since then many theoretical and practical papers alike, as well as vivid discussions, were dedicated to this topic [3–5]. The ability to effectively detect entangled state became essential mainly because of their application potential in quantum computing [6], quantum cryptography [7], and quantum teleportation experiments [8]. The most robust way of detecting it is via a full state tomography and density matrix estimation [9]. This method allows us to obtain all information about the state and thus correctly detect entanglement. Unfortunately this method is experimentally demanding because the number of required projections grows exponentially with the dimension of Hilbert space. There is also a variety of other methods that do not rely on full-state tomography [10–30]. These methods include a wide range of linear entanglement witnesses [11–16] of the CHSH – Clauser Horne Shimony Holt type [10]. While for pure states, these methods give similar results, their outcomes might vary significantly when mixed states are considered. While requiring only a relatively few measurement configurations, these witnesses can not reliably function without some a priori information about the detected state. To circumvent this limitation, while not resorting to state tomography, non-linear entanglement witnesses have been proposed.

In 2011, Rudnicki *et al.* introduced a nonlinear en-

tanglement witness called *Collectibility* [24, 26]. For a visual demonstration of this concept [see Fig.1 (a)]. For 2-qubit states, this witness requires two simultaneously prepared copies of the investigated state. Then a Bell state projection is imposed on a pair of corresponding qubits from each copy and the remaining qubits are subjected to local measurements. For a general 2-qubit state, this requires a combination of 5 local projections and, thus, fewer measurement configuration than full quantum state tomography which includes at least 24 projections. One can further decrease the time needed for a QST if measurements can be performed in parallel on multiple copies of the investigated state. When dealing with unknown quantum states, collectibility can detect a much broader range of states compared to linear witnesses. Namely, it detects all pure entangled states. Unfortunately, it detects entanglement of only a fraction of mixed states. This shortcoming is characterized by a rather big Type-II error (false negative), as we show later. On the other hand, all states which are classified as entangled by this method are classified correctly (Type-I error is null, there are no false-positive classifications). We demonstrate that significant improvement can be reached when collective entanglement witnesses are devised using an artificial neural network. As demonstrated by Gao *et al.* [31] and other groups [32, 33], neural networks can be used to identify quantum states. However, only linear entanglement witnesses were considered which significantly limited the class of detected entangled states. Note that neural network-based linear witnesses share the same shortcomings with their analytical counterparts, which is the need for a prior information about the investigated state.

We train a neural network to classify quantum states by providing it with results of collective measurements and demonstrate its significantly better performance over collectibility and other similar non-linear witnesses for a general 2-qubit state as well as for real experimental data for a fixed number of measurement

---

\*Electronic address: jan.roik@upol.cz

†Electronic address: bartkiewicz@jointlab.upol.cz

‡Electronic address: antonin.cernoch@upol.cz

§Electronic address: k.lemr@upol.cz

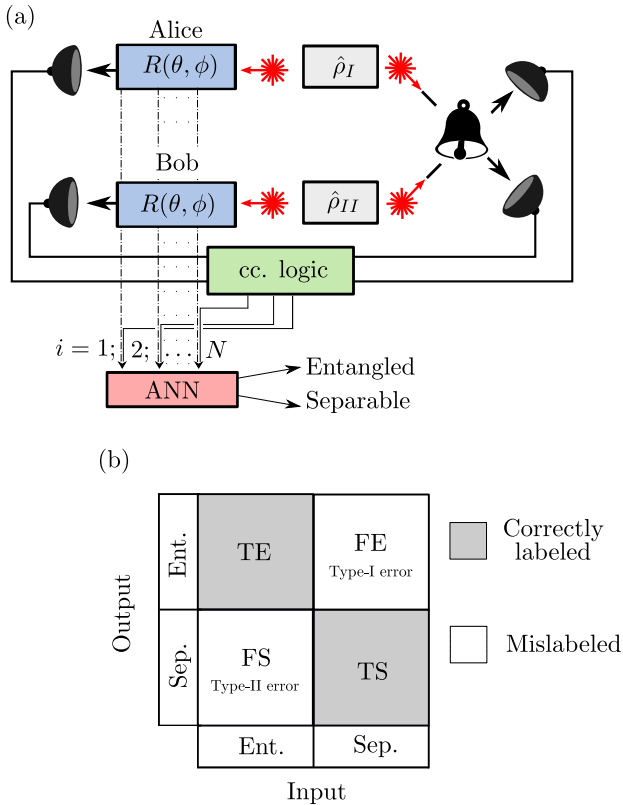


FIG. 1: (a) Scheme of collectibility measurement: Two copies  $\hat{\rho}_I, \hat{\rho}_{II}$  of the same quantum state are generated. One qubit from each pair is measured locally meanwhile remaining qubits are subjected to Bell measurement. Collectibility is then calculated analytically from obtained coincidence detections. Alternatively, as we investigate in this paper, coincidence detections can be fed to an ANN (artificial neural network) which then labels the states. (b) Schematic depiction of the confusion matrix used for performance evaluation of the ANN. TE – truly entangled, FE – falsely entangled, TS – truly separable, FS – falsely separable, Sep. – separable, Ent. – entangled.

configurations. Moreover, we show the increasing capability of the neural network when provided with a larger amount of measurement configuration outcomes by comparing it against three other analytical methods that require 12 projections, namely FEF – fully entangled fraction [34–36], CHSH [10], and entropic witness [37, 38]. These projections are listed in Appendix. We use confusion matrix as a method of performance evaluation for the ANN and previously known non-linear witnesses [see Fig.1 (b)]. Diagonal elements show the number of correctly labeled input states TE – truly entangled and TS – truly separable furthermore off-diagonal elements provide information about falsely labeled input states FE – falsely entangled and FS – falsely separable.

## II. NEURAL NETWORK

Random two-qubit states  $\hat{\rho}_I$  were generated (for more details see Appendix). The state of two of its copies is described by density matrix  $\hat{\rho}_I \otimes \hat{\rho}_{II}$  where  $\hat{\rho}_{II}$  is derived from  $\hat{\rho}_I$  by swapping subsystems. Subsequently, density matrix was subjected to projective measurements and probabilities were obtained

$$P_{xy} = \frac{\text{Tr}[(\hat{\rho}_I \otimes \hat{\rho}_{II})(\hat{\Pi}_x \otimes \hat{\Pi}_{\text{Bell}} \otimes \hat{\Pi}_y)]}{\text{Tr}[(\hat{\rho}_I \otimes \hat{\rho}_{II})(\hat{\Pi}_x \otimes \hat{\mathbb{1}}^{(4)} \otimes \hat{\Pi}_y)]}, \quad (1)$$

where  $\hat{\Pi}_x$  and  $\hat{\Pi}_y$  are local projections onto single-qubit states  $|x\rangle$  and  $|y\rangle$ ,  $\hat{\Pi}_{\text{Bell}}$  denotes projection onto the singlet Bell state and  $\hat{\mathbb{1}}^{(4)}$  represents four-dimensional identity matrix. Obtained set of  $N$  probabilities  $P_{xy}^{(i)}$ ;  $i = 1, \dots, N$  is subsequently fed to a neural network for training together with labels obtained by the PPT- Peres-Horodecki criterion [39, 40].

TensorFlow 2.0 [41] was used to program a neural network capable of classifying quantum states. We experimented with the complexity of the network and our final layout of the network with 5 hidden layers containing 36, 180, 75, 180, and 75 nodes respectively seems to be the optimal choice to find a balance between obtained precision and computation time. The proposed network is capable of assigning any quantum state with a value  $w \in [0; 1]$  which can be interpreted as a confidence factor from 0 (certainly entangled) to 1 (certainly separable). We defined decision threshold  $\epsilon$  to convert the  $w$  values to a binary label:  $w < \epsilon \Rightarrow$  entangled,  $w \geq \epsilon \Rightarrow$  separable. By changing  $\epsilon$  value we make the network biased towards the desired decision which allowed us to tune the trade-off between Type-I and Type-II errors. The network was trained on  $4 \times 10^6$  samples and tested on the other  $4 \times 10^5$  samples with distribution containing 67.74 % entangled states and 32.26 % separable states. For more details about the purity distribution of the samples see Appendix. The main goal was to test the network against collectibility, therefore, we start to train it using the same  $N = 5$  projection settings (see Appendix for a brief overview on collectibility). In the next step, we also tested capability of the network for  $N = 3, 6, 12, 15$  projection settings (see Appendix for more details).

## III. RESULTS

In the first step, we decided to test the neural network with decision threshold  $\epsilon = 0.5$  for a several amounts of projection settings  $N = 3, 5, 6, 12, 15$ . As it turns out the neural network was capable of labeling entangled and separable states even using 3 projection settings with an overall success rate of around 83.33 %. For an increasing number of projection settings success rate increased even further and reached 96.55 % for 15 projec-



ANN					
N	3	5	6	12	15
Type-I error (%)	0.93	0.96	1.18	0.24	0.22
Type-II error (%)	33.47	20.91	15.88	7.74	5.24
Success rate (%)	65.50	78.14	82.94	92.01	94.54

Collectibility				
N	5	12	12	12
Type-I error (%)	0	0	0	0
Type-II error (%)	63.41	14.00	42.00	54.00
Success rate (%)	36.59	86.00	58.00	46.00

TABLE I: Comparison of the results obtained by ANN for  $N = 3, 5, 6, 12, 15$  with prominent analytical methods (collectibility, FEF – fully entangled fraction, EW – entropic witness, CHSH nonlocality). Both Type-I and Type-II errors are taken for decision threshold  $\epsilon = 0.9$  to ensure Type-I error  $< 1\%$ .

arbitrary small by lowering the threshold value of  $W_N$  for classifying a given state as entangled.

#### IV. EXPERIMENTAL IMPLEMENTATION

To verify the network capability we decided to further test it on a set of real experimental data. For this purpose, we used the data set from the first-ever Collectibility measurement from 2016 [42]. In that particular experiment, a class of Werner states of the form of  $\hat{\rho}_w = p|\psi^-\rangle\langle\psi^-| + (1-p)\hat{1}/4$ , was investigated.  $|\psi^-\rangle$  represents singlet Bell state, and  $\hat{1}/4$  stands for the maximally mixed state. We set the detection threshold to  $\epsilon = 0.9$  like in the previous comparisons of the neural network with collectibility, to be consistent and make test conditions as fair as possible. Results show that collectibility can classify states with  $p > 0.89$  as entangled which corresponds with its theoretical prediction. The neural network, on the other hand, detects entangled states when  $p > 0.44$  (see Fig.4). Note that it is known that Werner states are entangled for  $p > \frac{1}{3}$ .

#### V. CONCLUSIONS

We trained a neural network to classify general qubit states based on nonlinear collective witnesses. Our main goal was to compare the capability of this network against a prominent analytical representation of nonlinear witnesses: the collectibility. The network can classify the general two-qubit states significantly more efficiently than collectibility with Type-I error  $< 1\%$ . The ANN also surpasses FEF, CHSH, and entropic witness when taught on 12 projections (the same amount needed by the mentioned analytical witnesses). Increasing the number of projection settings improves the ANN's decision even more. We further support this claim by using the network on a real experimental data set. The network confirmed its potential by cor-

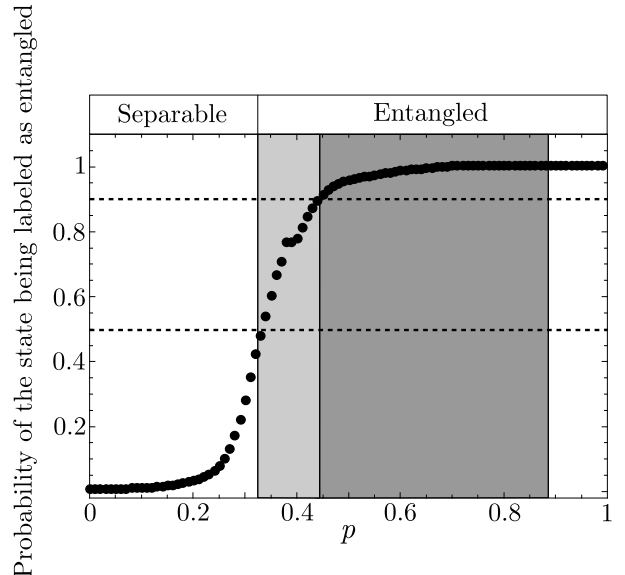


FIG. 4: Results obtained by neural network and collectibility respectively from a real experimental data set  $N = 5$ . Black full dots show the probability of a Werner state being labeled as entangled by the ANN. The light-gray area covers the values of  $p$  which neither the neural network nor collectibility can classify correctly. The dark-gray area represents the range of  $p$  values for which the ANN classifies the Werner states correctly and collectibility fails. The dashed lines represent the decision thresholds  $\epsilon = 0.9$  and  $0.5$  respectively.

rectly labeling a broad range of states where collectibility fails. Moreover, it achieved a Type-I error = 0 on Werner states. Our research promotes the idea of using artificial intelligence towards a better understanding of the intriguing physical phenomena such as the entanglement. We have demonstrated that the neural network can quickly train to become a valid efficient collective entanglement witness. We have directly compared its performance with analytical formulas. Using nonlinear measurements (on two copies of the state), our network operates completely free of any a priori information that can bias comparison of its performance with analytical counterparts. Moreover, we have shown that the training performed on numerically generated states works very well on real experimental data corresponding to states completely unknown to the ANN.

Because of technical limitations on the possible complexity of our ANN and on the number of samples processed in ANN training, reaching the limit of zero Type-I error was not possible. However, we were able to tune this error to a fraction of a percent by choosing a proper value of  $\epsilon$ . By extrapolating our results for the whole available range of  $\epsilon$ , we conclude that the limit of vanishing Type-I error is reached by the ANN for  $\epsilon = 0.9822$  and  $\epsilon = 0.9994$  for 5 and 12 measurements, respectively. The Type-II errors for these values of  $\epsilon$  are 31.26% (5 measurements, about 32% better than collectibility)

and 11.40% (12 measurements, 2.6% better than FEF). Thus, we have demonstrated that the best known analytical methods for certifying entanglement with a few measurements can be further improved. Notably, the 2.6% smaller Type-I error of ANN with respect to FEF, means that ANN fails relatively on about 20 % less states than FEF using the same input. This demonstrates that there is still a place for improvement in the theory of experimentally-friendly entanglement detection. The extrapolation of functional the dependence of Type-I and II errors on  $\epsilon$  was performed by fitting a quadratic and an exponential curve, respectively. We believe that the high quality of both fits and the proximity of the lowest Type-I error data point to 0 justify our conclusions. We hope that our results will stimulate further research in experimentally-friendly methods of classifying quantum states.

Further to that, the theoretical assumption of zero Type-I error of analytical witnesses does not hold operationally because of unavoidable experimental imperfections and finite precision of all measurements. As a result, separable states close to the decision boundary may be misclassified even using theoretically infallible witnesses. In this study, we have allowed the ANN a Type-I error of about 1 % which we believe is still an admissible error that can be tolerated in practical implementations burdened by the above-mentioned experimental imperfections. Note that in case of 12 measurement configurations, the ANN misclassifies only 1 in about 400 separable states while simultaneously misclassifying about two times less entangled states than its best performing analytical counterpart, the FEF.

### Acknowledgement

Authors thank Cesnet for providing data management services. Authors acknowledge financial support by the Czech Science Foundation under the project No. 19-19002S. KB also acknowledges the financial support of the Polish National Science Center under grant No. DEC-2019/34/A/ST2/00081. JR also acknowledges internal Palacky University grant IGA-PrF-2020-007. The authors also acknowledge the project No. CZ.02.1.01./0.0/0.0/16\_019/0000754 of the Ministry of Education, Youth and Sports of the Czech Republic. The attached digital supplement contains source codes, experimental data, and parameters of the artificial neural networks.

## Appendix: Theoretical framework

### A. State sampling and numerical processing

This paper focuses on general 2-qubit states. In order to correctly prepare test and training data sets, we generate diagonal elements of the  $4 \times 4$  matrix  $M$  according

to [43]:

$$M = \begin{pmatrix} M_{11} & 0 & 0 & 0 \\ 0 & M_{22} & 0 & 0 \\ 0 & 0 & M_{33} & 0 \\ 0 & 0 & 0 & M_{44} \end{pmatrix} \quad (3)$$

where  $M_{11} = r_1$ ;  $M_{22} = r_2(1 - M_{11})$ ;  $M_{33} = r_3(1 - M_{11} - M_{22})$ ;  $M_{44} = r_4(1 - M_{11} - M_{22} - M_{33})$ ;  $r_n$  for  $n = 1, 2, 3, 4$  gives uniformly distributed random numbers from range  $[0, 1]$ . The matrix is then normalized. In the next step, proper random unitary transformation was used in order to create a density matrix of general random 2-qubit state [44]

$$U = \begin{pmatrix} 1 & 0 & 0 & 0 \\ 0 & 1 & 0 & 0 \\ 0 & 0 & U_1 & \\ 0 & 0 & 0 & 1 \end{pmatrix} \begin{pmatrix} 1 & 0 & 0 & 0 \\ 0 & U_2 & 0 & \\ 0 & 0 & 0 & 1 \\ 0 & 0 & 0 & 1 \end{pmatrix} \begin{pmatrix} U_3 & 0 & 0 \\ 0 & 0 & 1 & 0 \\ 0 & 0 & 0 & 1 \end{pmatrix} \quad (4)$$

$$\begin{pmatrix} 1 & 0 & 0 & 0 \\ 0 & 1 & 0 & 0 \\ 0 & 0 & U_4 & \\ 0 & 0 & 0 & 1 \end{pmatrix} \begin{pmatrix} 1 & 0 & 0 & 0 \\ 0 & U_5 & 0 & \\ 0 & 0 & 0 & 1 \\ 0 & 0 & 0 & 1 \end{pmatrix} \begin{pmatrix} 1 & 0 & 0 & 0 \\ 0 & 1 & 0 & 0 \\ 0 & 0 & U_6 & \\ 0 & 0 & 0 & 1 \end{pmatrix},$$

where

$$U_j = e^{i\alpha_j} \begin{pmatrix} e^{i\psi_j} \cos \phi_j & e^{i\chi_j} \sin \phi_j \\ -e^{-i\chi_j} \sin \phi_j & e^{-i\psi_j} \cos \phi_j \end{pmatrix}, \quad j = 1, \dots, 6 \quad (5)$$

with  $0 \leq \phi \leq \frac{\pi}{2}$ ,  $0 \leq \alpha, \psi, \chi < 2\pi$ . The homogenous distribution of states was ensured by  $\phi_j = \arcsin \sqrt{\xi_j}$ ,  $\xi_j \in [0, 1]$ . Parameters  $\phi_j, \psi_j, \chi_j, \alpha_j$  and  $\xi_j$  are picked from their respective intervals with uniform probability. The final density matrix was obtained as  $M_o = U M U^\dagger$ . Training and test data were labeled via PPT criterion [39, 40]. To mathematically describe the collective measurement a 4-qubit density matrix  $M_f$  was defined as  $M_f = M_o \otimes M_t$ . To implement Bell-state projection on the neighboring (2,3) qubits,  $M_t$  is obtained from  $M_o$  by switching subsystems

$$M_t = \text{SWAP } M_o \text{ SWAP}, \quad (6)$$

where

$$\text{SWAP} = \begin{pmatrix} 1 & 0 & 0 & 0 \\ 0 & 0 & 1 & 0 \\ 0 & 1 & 0 & 0 \\ 0 & 0 & 0 & 1 \end{pmatrix}. \quad (7)$$

### B. Collectibility

In order to calculate collectibility we used the formula by Rudnický *et al.* [26] represented in computational bases, i.e.,  $H \rightarrow |0\rangle$ ;  $V \rightarrow |1\rangle$ ;  $D \rightarrow |+\rangle = (|0\rangle +$

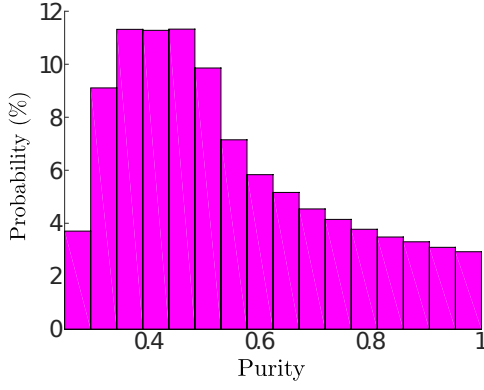


FIG. 5: Purity distribution of the training and test states.

$|1\rangle)/\sqrt{2}$ ;  $A \rightarrow |-\rangle = (|0\rangle - |1\rangle)/\sqrt{2}$ ;  $R \rightarrow (|0\rangle - i|1\rangle)/\sqrt{2}$   
and,  $L \rightarrow (|0\rangle + i|1\rangle)/\sqrt{2}$

$$W(\hat{\rho}) = \frac{1}{2}[\eta + p_0^2(1 - r_{00}) + (1 - p_0)^2(1 - r_{11}) + 2p_0(1 - p_0)(1 - r_{01}) - 1], \quad (8)$$

where

$$\eta = 8p_0(1 - p_0)\sqrt{r_{00}r_{11}} + 2p^j. \quad (9)$$

In the equations above single-photon projection probability  $p_0 = M_{o_{00}} + M_{o_{11}}$  and  $p^j = \max\{p_{++}, p_{--}\}$ .  $P_{xy}$  represents probabilities of single Bell state projection of non-locally measured qubit conditioned on local projection onto  $|x\rangle$  and  $|y\rangle$  states.[26]

### C. Other two-copy witnesses.

A class of two-copy entanglement witnesses can be calculated using elements of the symmetric matrix [35]

$$R_{i,j} = R_{j,i} = \langle \sigma_i^{(a_1)} \otimes \sigma_j^{(a_2)} \otimes |\Psi_{b_1, b_2}^-\rangle \langle \Psi_{b_1, b_2}^-| \rangle, \quad (10)$$

where the expectation values are calculated on two copies of  $\rho$ , i.e.,  $\rho_{a_1, b_1} \otimes \rho_{a_2, b_2}$ . To estimate the number of projections let use the resolution of two-qubit identity operator valid for an arbitrary  $i, j = 1, 2, 3$ , which reads

$$\mathbb{1}^{\otimes 2} = \sum_{r,s=0,1} |r_i s_j\rangle \langle r_i s_j|, \quad (11)$$

where  $|0_i\rangle$  and  $|1_i\rangle$  are eigenstates of  $\sigma_i$  operator associated with  $\pm 1$  eigenvalues, respectively. A product of two Pauli operators reads

$$\sigma_i^{(a_1)} \otimes \sigma_j^{(a_2)} = |0_i 0_j\rangle \langle 0_i 0_j| + |1_i 1_j\rangle \langle 1_i 1_j| - (|0_i 1_j\rangle \langle 0_i 1_j| + |1_i 0_j\rangle \langle 1_i 0_j|). \quad (12)$$

N	$ i\rangle j\rangle$
3	$ H\rangle H\rangle,  V\rangle V\rangle,  H\rangle V\rangle$
5	$ H\rangle H\rangle,  V\rangle V\rangle,  H\rangle V\rangle,  D\rangle D\rangle,  A\rangle A\rangle$
6	$ H\rangle H\rangle,  V\rangle V\rangle,  H\rangle V\rangle,  D\rangle D\rangle,  R\rangle R\rangle,  L\rangle L\rangle$
12	$ D\rangle D\rangle,  A\rangle A\rangle,  D\rangle L\rangle,  A\rangle R\rangle,  D\rangle H\rangle,  A\rangle V\rangle,  L\rangle L\rangle,  R\rangle R\rangle,  L\rangle H\rangle,  R\rangle V\rangle,  H\rangle H\rangle,  V\rangle V\rangle,$
15	$ D\rangle D\rangle,  A\rangle A\rangle,  D\rangle L\rangle,  A\rangle R\rangle,  D\rangle H\rangle,  A\rangle V\rangle,  L\rangle L\rangle,  R\rangle R\rangle,  L\rangle H\rangle,  R\rangle V\rangle,  H\rangle H\rangle,  V\rangle V\rangle,  D\rangle R\rangle,  D\rangle V\rangle,  L\rangle V\rangle$

TABLE II: List of specific projections settings used for the learning of the artificial neural network.

By adding the corresponding sides of Eq. (11) to Eq. (12) and subtracting  $\mathbb{1}^{\otimes 2}$  we obtain

$$\sigma_i^{(a_1)} \otimes \sigma_j^{(a_2)} = 2(|0_i 0_j\rangle \langle 0_i 0_j| + |1_i 1_j\rangle \langle 1_i 1_j|) - \mathbb{1}^{\otimes 2}. \quad (13)$$

This means that measuring all 6 different elements of  $R$  (i.e.,  $i \leq j$  for  $i, j = 1, 2, 3$ ) requires 12 projections in total. These projections read

$$\begin{aligned} &|D\rangle|D\rangle, |A\rangle|A\rangle, |D\rangle|L\rangle, |A\rangle|R\rangle, \\ &|D\rangle|H\rangle, |A\rangle|V\rangle, |L\rangle|L\rangle, |R\rangle|R\rangle, \\ &|L\rangle|H\rangle, |R\rangle|V\rangle, |H\rangle|H\rangle, |V\rangle|V\rangle. \end{aligned} \quad (14)$$

By using these 12 projections we determine matrix  $Q$  used to calculate entanglement witnesses. Fully entangled fraction  $f$  can be used to construct an entanglement witness [35]

$$F = 2f - 1 = \frac{1}{2}[\text{Tr}(\sqrt{Q}) - 1]. \quad (15)$$

This and the following witnesses are positive, if entanglement is detected and negative, otherwise. The maximum value is 1.

Furthermore, by using an optimal CHSH inequality we can construct an entanglement witness [35] as

$$M = \text{Tr}(Q) - \min[\text{eig}(Q)]. \quad (16)$$

It is also possible to use  $Q$  to express an entropic entanglement witness [35]

$$E = \frac{1}{2}[\text{Tr}(Q) - 1]. \quad (17)$$

N	3		5		6		12		15	
	T-I	T-II	T-I	T-II	T-I	T-II	T-I	T-II	T-I	T-II
0.5	9.23	7.42	7.09	4.98	5.47	5.03	2.17	2.43	1.50	1.94
0.55	8.03	8.84	6.17	5.91	4.77	5.83	1.34	3.55	1.27	2.19
0.6	6.94	10.49	5.32	6.97	4.14	6.73	1.15	3.89	1.06	2.48
0.65	5.87	12.38	4.48	8.24	3.47	7.94	0.97	4.31	0.86	2.82
0.7	4.81	14.65	3.72	9.73	2.94	9.12	0.81	4.76	0.67	3.22
0.75	3.73	17.64	3.18	10.97	2.53	10.17	0.66	5.29	0.50	3.71
0.8	2.75	21.37	1.93	15.05	2.12	11.51	0.51	5.91	0.41	4.07
0.85	1.72	26.79	1.47	17.38	1.67	13.28	0.37	6.68	0.32	4.53
0.9	0.93	33.47	0.96	20.91	1.18	15.88	0.24	7.75	0.22	5.24
0.95	0.41	41.21	0.42	27.42	0.63	20.41	0.11	9.61	0.11	6.77

TABLE III: Evolution of Type-I and Type-II error for different thresholds  $\epsilon$ . T-I and T-II represent Type-I and Type-II errors respectively and are listed in percentages.

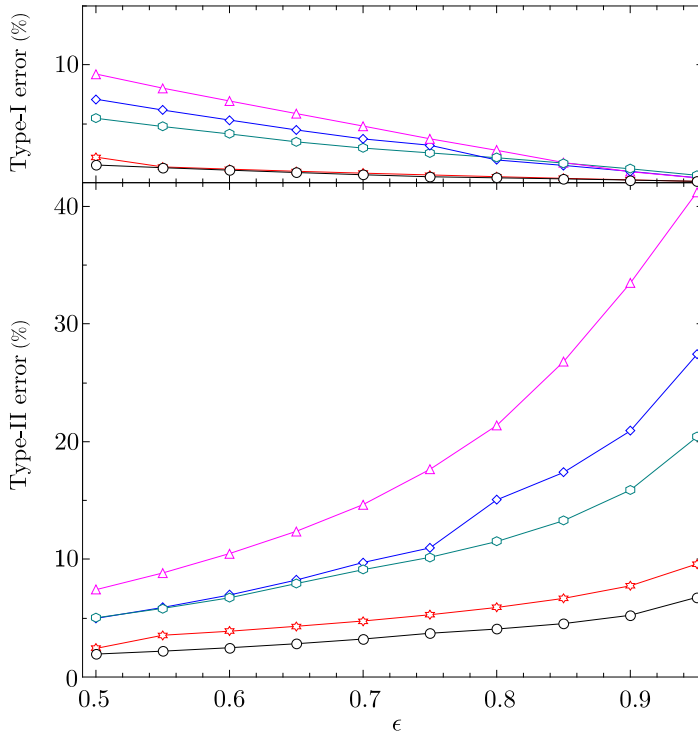


FIG. 6: Dependence of Type I and Type II errors on  $\epsilon$  threshold for varying numbers of projections: Three projection  $N = 3$  ( $\Delta$ ), five projections  $N = 5$  ( $\diamond$ ), six projections  $N = 6$  ( $\circ$ ), twelve projections  $N = 12$  ( $\star$ ), fifteen projections  $N = 15$  ( $\circ$ ).

- 
- [1] E. Schrödinger, “Discussion of probability relations between separated systems,” *Mathematical Proceedings of the Cambridge Philosophical Society*, vol. 31, no. 4, p. 555–563, 1935.
- [2] A. Einstein, B. Podolsky, and N. Rosen, “Can quantum-mechanical description of physical reality be considered complete?,” *Phys. Rev.*, vol. 47, pp. 777–780, May 1935.
- [3] M. B. Plenio and S. Virmani, “An introduction to entanglement theory,” in *Quantum Information and Coherence*, pp. 173–209, Springer, 2014.
- [4] R. Horodecki, P. Horodecki, M. Horodecki, and K. Horodecki, “Quantum entanglement,” *Rev. Mod. Phys.*, vol. 81, pp. 865–942, Jun 2009.
- [5] F. Mintert, A. Carvalho, M. Kuś, and A. Buchleitner, “Measures and dynamics of entangled states,” *Physics Reports*, vol. 415, no. 4, pp. 207–259, 2005.
- [6] A. Steane, “Quantum computing,” *Reports on Progress in Physics*, vol. 61, pp. 117–173, feb 1998.
- [7] N. Gisin, G. Ribordy, W. Tittel, and H. Zbinden, “Quantum cryptography,” *Rev. Mod. Phys.*, vol. 74, pp. 145–195, Mar 2002.
- [8] D. Bouwmeester, J.-W. Pan, K. Mattle, M. Eibl, H. Weinfurter, and A. Zeilinger, “Experimental quantum teleportation,” *Nature*, vol. 390, pp. 575–579, Dec 1997.
- [9] A. Salles, F. de Melo, M. P. Almeida, M. Hor-Meyll, S. P. Walborn, P. H. Souto Ribeiro, and L. Davidovich, “Experimental investigation of the dynamics of entanglement: Sudden death, complementarity, and continuous monitoring of the environment,” *Phys. Rev. A*, vol. 78, p. 022322, Aug 2008.
- [10] J. F. Clauser, M. A. Horne, A. Shimony, and R. A. Holt, “Proposed experiment to test local hidden-variable theories,” *Phys. Rev. Lett.*, vol. 23, pp. 880–884, Oct 1969.
- [11] K. Bartkiewicz, B. Horst, K. Lemr, and A. Miranowicz, “Entanglement estimation from Bell inequality violation,” *Phys. Rev. A*, vol. 88, p. 052105, Nov 2013.
- [12] P. Horodecki, “From limits of quantum operations to multicopy entanglement witnesses and state-spectrum estimation,” *Phys. Rev. A*, vol. 68, p. 052101, Nov 2003.
- [13] F. A. Bovino, G. Castagnoli, A. Ekert, P. Horodecki, C. M. Alves, and A. V. Sergienko, “Direct measurement of nonlinear properties of bipartite quantum states,” *Phys. Rev. Lett.*, vol. 95, p. 240407, Dec 2005.
- [14] A. R. R. Carvalho, F. Mintert, and A. Buchleitner, “Decoherence and multipartite entanglement,” *Phys. Rev. Lett.*, vol. 93, p. 230501, Dec 2004.
- [15] Z.-H. Chen, Z.-H. Ma, O. Gühne, and S. Severini, “Estimating entanglement monotones with a generalization of the Wootters formula,” *Phys. Rev. Lett.*, vol. 109, p. 200503, Nov 2012.
- [16] L. Aolita and F. Mintert, “Measuring multipartite concurrence with a single factorizable observable,” *Phys. Rev.*

- Lett.*, vol. 97, p. 050501, Aug 2006.
- [17] S. P. Walborn, P. H. Souto Ribeiro, L. Davidovich, F. Mintert, and A. Buchleitner, “Experimental determination of entanglement with a single measurement,” *Nature*, vol. 440, pp. 1022–1024, Apr 2006.
- [18] P. Badziąg, i. c. v. Brukner, W. Laskowski, T. Paterek, and M. Żukowski, “Experimentally friendly geometrical criteria for entanglement,” *Phys. Rev. Lett.*, vol. 100, p. 140403, Apr 2008.
- [19] M. Huber, F. Mintert, A. Gabriel, and B. C. Hiesmayr, “Detection of high-dimensional genuine multipartite entanglement of mixed states,” *Phys. Rev. Lett.*, vol. 104, p. 210501, May 2010.
- [20] O. Gühne, M. Reimpell, and R. F. Werner, “Estimating entanglement measures in experiments,” *Phys. Rev. Lett.*, vol. 98, p. 110502, Mar 2007.
- [21] J. Eisert, F. G. S. L. Brandão, and K. M. R. Audenaert, “Quantitative entanglement witnesses,” *New Journal of Physics*, vol. 9, pp. 46–46, mar 2007.
- [22] R. Augusiak, M. Demianowicz, and P. Horodecki, “Universal observable detecting all two-qubit entanglement and determinant-based separability tests,” *Phys. Rev. A*, vol. 77, p. 030301, Mar 2008.
- [23] A. Osterloh and P. Hyllus, “Estimating multipartite entanglement measures,” *Phys. Rev. A*, vol. 81, p. 022307, Feb 2010.
- [24] L. Rudnicki, P. Horodecki, and K. Życzkowski, “Collective uncertainty entanglement test,” *Phys. Rev. Lett.*, vol. 107, p. 150502, Oct 2011.
- [25] B. Jungnitsch, T. Moroder, and O. Gühne, “Taming multiparticle entanglement,” *Phys. Rev. Lett.*, vol. 106, p. 190502, May 2011.
- [26] L. Rudnicki, Z. Puchała, P. Horodecki, and K. Życzkowski, “Collectibility for mixed quantum states,” *Phys. Rev. A*, vol. 86, p. 062329, Dec 2012.
- [27] Ł. Rudnicki, Z. Puchała, P. Horodecki, and K. Życzkowski, “Constructive entanglement test from triangle inequality,” *Journal of Physics A: Mathematical and Theoretical*, vol. 47, p. 424035, oct 2014.
- [28] L. Zhou and Y.-B. Sheng, “Detection of nonlocal atomic entanglement assisted by single photons,” *Phys. Rev. A*, vol. 90, p. 024301, Aug 2014.
- [29] H. S. Park, S.-S. B. Lee, H. Kim, S.-K. Choi, and H.-S. Sim, “Construction of an optimal witness for unknown two-qubit entanglement,” *Phys. Rev. Lett.*, vol. 105, p. 230404, Dec 2010.
- [30] W. Laskowski, D. Richart, C. Schwemmer, T. Paterek, and H. Weinfurter, “Experimental Schmidt decomposition and state independent entanglement detection,” *Phys. Rev. Lett.*, vol. 108, p. 240501, Jun 2012.
- [31] J. Gao, L.-F. Qiao, Z.-Q. Jiao, Y.-C. Ma, C.-Q. Hu, R.-J. Ren, A.-L. Yang, H. Tang, M.-H. Yung, and X.-M. Jin, “Experimental machine learning of quantum states,” *Phys. Rev. Lett.*, vol. 120, p. 240501, Jun 2018.
- [32] Y.-C. Ma and M.-H. Yung, “Transforming Bell’s inequalities into state classifiers with machine learning,” *npj Quantum Information*, vol. 4, p. 34, Jul 2018.
- [33] S. Lu, S. Huang, K. Li, J. Li, J. Chen, D. Lu, Z. Ji, Y. Shen, D. Zhou, and B. Zeng, “Separability-entanglement classifier via machine learning,” *Phys. Rev. A*, vol. 98, p. 012315, Jul 2018.
- [34] C. H. Bennett, D. P. DiVincenzo, J. A. Smolin, and W. K. Wootters, “Mixed-state entanglement and quantum error correction,” *Phys. Rev. A*, vol. 54, pp. 3824–3851, Nov 1996.
- [35] K. Bartkiewicz, K. Lemr, A. Černocho, and A. Miranowicz, “Bell nonlocality and fully entangled fraction measured in an entanglement-swapping device without quantum state tomography,” *Phys. Rev. A*, vol. 95, p. 030102, Mar 2017.
- [36] K. Bartkiewicz, P. Horodecki, K. Lemr, A. Miranowicz, and K. Życzkowski, “Method for universal detection of two-photon polarization entanglement,” *Phys. Rev. A*, vol. 91, p. 032315, Mar 2015.
- [37] A. S. M. de Castro and V. V. Dodonov, “Covariance measures of intermode correlations and inseparability for continuous variable quantum systems,” *Journal of Optics B: Quantum and Semiclassical Optics*, vol. 5, pp. S593–S608, oct 2003.
- [38] V. Vedral and M. B. Plenio, “Entanglement measures and purification procedures,” *Phys. Rev. A*, vol. 57, pp. 1619–1633, Mar 1998.
- [39] M. Horodecki, P. Horodecki, and R. Horodecki, “Separability of mixed states: necessary and sufficient conditions,” *Physics Letters A*, vol. 223, no. 1, pp. 1–8, 1996.
- [40] A. Peres, “Separability criterion for density matrices,” *Phys. Rev. Lett.*, vol. 77, pp. 1413–1415, Aug 1996.
- [41] M. Abadi, P. Barham, J. Chen, Z. Chen, A. Davis, J. Dean, M. Devin, S. Ghemawat, G. Irving, M. Isard, *et al.*, “Tensorflow: A system for large-scale machine learning,” in *12th {USENIX} symposium on operating systems design and implementation ({OSDI} 16)*, pp. 265–283, 2016.
- [42] K. Lemr, K. Bartkiewicz, and A. Černocho, “Experimental measurement of collective nonlinear entanglement witness for two qubits,” *Phys. Rev. A*, vol. 94, p. 052334, Nov 2016.
- [43] J. Maziero, “Random sampling of quantum states: a survey of methods,” *Brazilian Journal of Physics*, vol. 45, pp. 575–583, Dec 2015.
- [44] C.-K. LI, R. ROBERTS, and X. YIN, “Decomposition of unitary matrices and quantum gates,” *International Journal of Quantum Information*, vol. 11, no. 01, p. 1350015, 2013.